Laser spectroscopy of Nd^{3+} ions in GeO_2-PbO-Bi_2O_3 glasses

R. Balda, J. Fernández, and M. Sanz
Departamento de Física Aplicada I, ETSII y Telecomunicación, Universidad del País Vasco, Alameda Urquijo s/n, 48013, Bilbao, Spain

A. de Pablos and J. M. Fdez-Navarro
Instituto de Cerámica y Vidrio, 28500 Arganda del Rey, Madrid, Spain

J. Mugnier
Laboratoire de Physico-Chimie des Materiaux Luminescents, UMR No. 5620, Université Claude Bernard Lyon 1, 69622 Villeurbanne Cedex, France

(Received 11 August 1999; revised manuscript received 12 October 1999)

The optical properties of Nd^{3+} ions in six different compositions of glasses based on GeO_2, PbO, and Bi_2O_3 have been investigated by using steady-state and time-resolved laser spectroscopy. Judd-Ofelt parameters were derived from the absorption spectra and used to calculate the $^4F_{3/2}\rightarrow{}^4I_{11/2}$ stimulated emission cross section and the $^4F_{3/2}$ radiative lifetime. Site-selective spectroscopy and time resolved fluorescence line narrowing experiments were performed in the $^4F_{3/2}\rightarrow{}^4I_{9/2}$, $^4I_{11/2}$ transitions. For all samples studied a line narrowing of the $^4F_{3/2}\rightarrow{}^4I_{11/2}$ emission has been observed when exciting at the long wave side of the $^4I_{9/2}\rightarrow{}^4F_{3/2}$ transition. The lifetimes of the $^4F_{3/2}$ state do not show a monotonic variation with the excitation wavelength indicating large site-to-site variations in the local crystal field. Spectral migration of excitation among the Nd^{3+} ions has been studied from the time evolution of the $^4F_{3/2}\rightarrow{}^4I_{9/2}$ spectra under resonant excitation. The results can be interpreted in terms of a dipole-dipole energy transfer mechanism. Visible upconversion has been observed in these glasses under infrared laser excitation.

I. INTRODUCTION

Glasses based on heavy metal oxides are becoming an important class of materials for optoelectronics applications, especially because of their high refractive index and low phonon energies.[1–3] The reduced phonon energy increases the quantum efficiency of luminescence from excited states of rare earth ions in these matrices and provides the possibility to develop more efficient lasers and fiber optics amplifiers at longer wavelengths than available from other oxide glasses.[4] Among the different compositions studied, lead germanate glasses combine high mechanical strength, high chemical durability, and temperature stability with good transmission in the infrared region[5] up to 4.5 μm, which make them promising materials for technological applications such as new lasing materials, upconverting phosphors, and optical waveguides.[6–10] To develop oxide glasses with extended infrared transmittance, large cations with low field strength can be added. Germania based glasses containing lead and bismuth oxides are most suitable for such optical waveguide materials. Recently, Miller *et al.* observed that glasses in the GeO_2-PbO-Bi_2O_3 system have significantly higher Raman scattering cross sections than silica-based compositions,[11] which make them potential candidates for fiber optic amplifiers and oscillators by using stimulated Raman scattering.[12]

The optical properties of rare-earth ions in glasses depend on the chemical composition of the glass matrix, which determines the structure and nature of the bonds.[13] The development of new glass-based optical devices requires a better understanding of the interionic interactions which are deeply involved in the fundamental physics of rare earth ions. Although rare earths are not randomly distributed throughout the glass and they may or may not enter as former ions, their optical spectra show, even at low concentrations, an inhomogeneous broadening which is the evidence of large site-to-site crystal field variations. Several laser spectroscopic techniques, such as fluorescence line narrowing (FLN), spectral hole burning, etc.,[14,15] are required to obtain detailed information on the local field and ion-ion and ion-host interaction processes.

Among the various rare-earth ions, neodymium is the most widely studied ion in a variety of glasses not only because of its applications, but also because the variations with composition of its spectroscopic properties usually apply to other trivalent rare earth ions.[13] These properties include absorption and emission cross sections, peak wavelengths, and linewidths, lifetimes and quantum efficiencies, and fluorescence quenching processes. To achieve the highest efficiency, fluorescence lifetimes of Nd^{3+} ions must closely approach the calculated radiative lifetime which is determined by all the competing radiative and nonradiative decay processes; the latter include both Nd-Nd self-quenching and multiphonon relaxation. Concentration quenching and multiphonon emission are dependent on the RE ion and the glass hosts.[16]

In this work we report the optical properties of Nd^{3+} ions in six different compositions of binary and ternary glasses based on GeO_2, PbO, and Bi_2O_3. To the best knowledge of the authors, there is no detailed study of the optical properties of Nd^{3+} in these glasses. A recent work by Wachtler *et al.*[10] reports a basic optical characterization of Nd^{3+} ions in a binary lead-germanate glass. The present study includes absorption and emission properties, site-selective spectroscopy, time-resolved fluorescence line narrowing experiments, and infrared to visible upconversion. In order to establish a correlation between glass matrix composition and Nd^{3+} spectral properties, steady-state site selective and reso-

TABLE I. Nominal composition (mol %) and density ($g\,cm^{-3}$) of the samples studied.

Glass	Composition (mol %)	d ($g\,cm^{-3}$)
GP	$59GeO_2$-41PbO	6.21
GPB1	$62.5GeO_2$-12.5PbO-$25Bi_2O_3$	6.65
GPB2	$58.82GeO_2$-23.53PbO-$17.65Bi_2O_3$	6.63
GPB3	$55.56GeO_2$-33.33PbO-$11.11Bi_2O_3$	6.52
GPB4	$52.63GeO_2$-42.11PbO-$5.26Bi_2O_3$	6.53
GB	$75GeO_2$-$25Bi_2O_3$	6.22

nant time-resolved fluorescence line narrowing (TRFLN) spectroscopy were performed to obtain information about the site distribution of Nd^{3+} ions and the energy transfer among them. It is worthwhile mentioning that TRFLN techniques have only been used in a few studies on spectral diffusion among Nd^{3+} ions in glasses;[17–21] among these, there are only a few works performed in a resonant pumping scheme[20,21] to excite the $^4F_{3/2}$ state of Nd^{3+} ions.

II. EXPERIMENTAL TECHNIQUES

Batches of 20 g of glass have been prepared by mixing high purity reagents GeO_2 (ALFA 99.999), PbO (ALFA 99.9995), Bi_2O_3 (ALFA 99.999); all glasses were doped with 1% Nd_2O_3 (ALFA 99.999). This mixture was melted in a high purity alumina crucible placed in a vertical tubular furnace at a temperature between 1100–1200 °C for 1 h and then poured onto a preheated brass plate, followed by 1 h annealing at 420 °C and cooling at 1.5 °C/min down to room temperature. Finally the samples were cut and polished for optical measurements. The composition and density of the glasses in the system GeO_2-PbO-Bi_2O_3 are listed in Table I.

The samples temperature was varied between 4.2 and 300 K in a continuous flow cryostat. Conventional absorption spectra were performed with a Cary 5 spectrophotometer. The emission measurements were made by using an argon laser and a Ti-sapphire ring laser (0.4 cm^{-1} linewidth) in the 780–920 nm range. The fluorescence was analyzed with a 0.22 m SPEX monochromator, and the signal was detected by a Hamamatsu R7102 extended IR photomultiplier and finally amplified by a standard lock-in technique. The visible fluorescence was detected by a Hamamatsu R928 photomultiplier.

Lifetime measurements and time resolved resonant fluorescence line narrowed emission measurements were obtained by exciting the samples with a Ti-sapphire laser, pumped by a pulsed frequency doubled Nd:YAG laser (9 ns pulse width), and detecting the emission with a Hamamatsu R7102 photomultiplier and with a Hamamatsu R5108 photomultiplier provided with a gating circuit designed to enable gate control from external applied TTL level control signal. Data were processed by an EGG-PAR boxcar integrator.

III. RESULTS AND DISCUSSION

A. Absorption and emission properties

The room temperature absorption spectra of Nd^{3+} in these glasses were recorded in the 300–2500 nm spectral range by using a Cary 5 spectrophotometer. The spectral resolution was 0.5 nm at wavelengths below 1100 nm, and 2 nm above. As an example, Fig. 1 shows the absorption coefficient for the six glasses doped with 1 mol % of Nd^{3+} in the 400–950 nm range. The position of the absorption bands are similar with slight differences in intensity. However, as expected, the UV absorption edge is shifted to longer wavelengths in the samples containing bismuth oxide.[22] Data from these spectra can be used to calculate the radiative lifetime of the $^4F_{3/2}$ excited J manifold, the branching ratios, and the radiative transition probabilities of fluorescence transitions to the lower lying ^4I_J manifolds, according to the Judd-Ofelt (JO) theory.[23,24] The JO parameters obtained for these glasses are displayed in Table II. These values are in good agreement with those previously reported for the Nd^{3+} ion in different glass materials.[4,10,25,26] Ω_2 is the most sensitive to local structure and glass composition and its value is indicative of the amount of covalent bonding.[27] As can be seen in Table II the Ω_2 value is higher for the samples with the higher amount of bismuth (glasses GPB1 and GB) which have a more covalent bonding character. Since the Ω_2 parameter reflects the asymmetry of the local environment at the Nd^{3+} site, a smaller value for glass GP suggests a more centrosymmetric coordination environment.

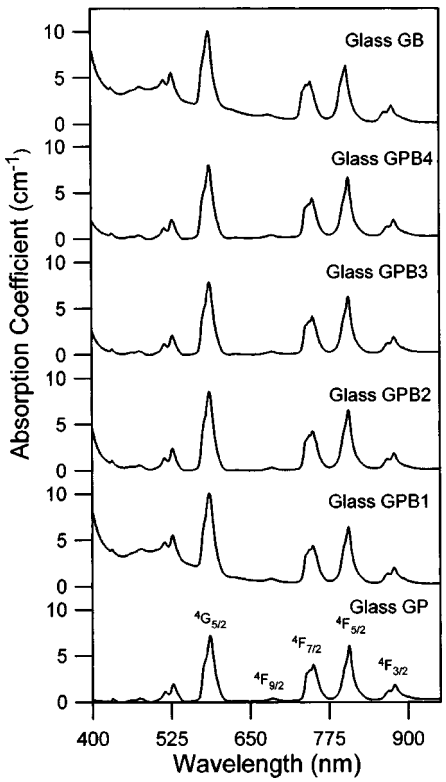

FIG. 1. Room temperature absorption spectra of Nd^{3+} ions in the six studied samples.

The spontaneous emission probabilities from the $^4F_{3/2}$ to the ^4I_J states were calculated from the JO parameters and used to obtain the radiative lifetimes.[28] The measured effective linewidth and the spontaneous emission probability of the $^4F_{3/2}\rightarrow{}^4I_{11/2}$ transition make it possible to evaluate the stimulated emission cross section[25] of this laser transition for all samples. The resulting radiative lifetime τ_R and the stimulated emission cross section for the $^4F_{3/2}\rightarrow{}^4I_{11/2}$ tran-

TABLE II. Judd-Ofelt parameters (10^{-20} cm^2) calculated from the absorption spectra of Nd^{3+} ions in bismuth lead-germanate glasses.

Glass	Ω_2	Ω_4	Ω_6	r.m.s. (10^{-7})
GP	2.95	5.01	3.93	4.74
GPB1	3.94	3.77	3.94	3.07
GPB2	3.43	5.01	3.86	6.23
GPB3	3.73	5.70	4.35	5.95
GPB4	3.22	5.01	3.90	4.97
GB	4.79	4.52	4.70	2.91

sition are presented in Table III together with the effective fluorescence linewidth and peak position. As can be seen, the fluorescence peak positions are similar in all samples ranging from 1063.7 to 1065 nm. The narrowest effective linewidth corresponds to glass GP, increasing as the bismuth oxide concentration increases in the glass composition. The stimulated emission cross section is determined by Ω_4, Ω_6, and the effective fluorescence linewidth. In this case the highest value corresponds to glass GPB3. The radiative lifetimes are in reasonable agreement with the experimental values; however for glasses GP, GPB2, and GPB3 the experimental lifetime is longer than the radiative one. This behavior has been observed in tellurite[29] and gallate glasses,[4] which may result because the calculated line strength of the $^4I_{9/2} \rightarrow {}^4F_{3/2}$ transition is larger than the measured line strength.[28]

B. Site-selective spectroscopy

Taking advantage of the tunability and narrow bandwidth of the Ti-sapphire ring laser as an excitation source for the $^4I_{9/2} \rightarrow {}^4F_{3/2}$ transition, we have performed the excitation spectra of this transition by collecting the luminescence at different wavelengths along the $^4F_{3/2} \rightarrow {}^4I_{11/2}$ transition. As an example Fig. 2 shows the steady-state excitation spectra for glass GPB2, obtained at two different emission wavelengths measured at 4.2 K. As can be observed the spectrum slightly narrows and blueshifts for emission at the high energy wing of the $^4F_{3/2} \rightarrow {}^4I_{11/2}$ emission.

The steady-state site selective emission spectra for the $^4F_{3/2} \rightarrow {}^4I_{11/2}$ transition were performed by exciting at different wavelengths in the low energy component of the $^4I_{9/2} \rightarrow {}^4F_{3/2}$ absorption band. Figure 3 shows the emission spectra of glass GP obtained at different excitation wavelengths measured at 4.2 K. As can be observed, as excitation wavelength increases along the low-energy Stark component of

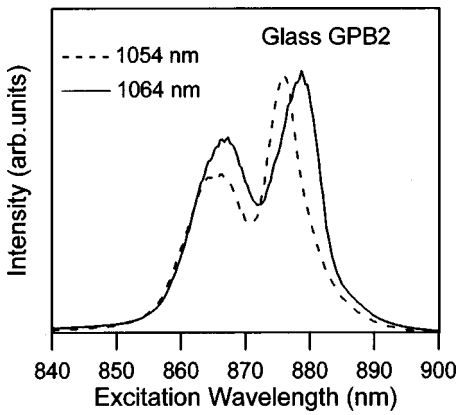

FIG. 2. Steady-state excitation spectra of $^4I_{9/2} \rightarrow {}^4F_{3/2}$ transition in glass GPB2 for luminescence monitored at two different wavelengths within the $^4F_{3/2} \rightarrow {}^4I_{11/2}$ emission band. Measurements were performed at 4.2 K.

the doubled $^4F_{3/2}$, the shape of the emission band changes and a narrowing and redshift of the emission spectra occurs. For all samples the spectra are characterized by fluorescence bands having poorly resolved components and a large residue of inhomogeneous broadening. However, the fluorescence spectra of glass GP show more resolved and slightly narrower lines which indicate a glass with a small site-to-site variation in the local field.

The decays of the $^4F_{3/2} \rightarrow {}^4I_{11/2}$ transition were obtained by exciting the samples at different wavelengths along the low energy component of the $^4I_{9/2} \rightarrow {}^4F_{3/2}$ absorption band. They were found to be single exponentials at all temperatures and compositions, to a good approximation. This behavior may be due to the use of narrow band laser excitation. Measurements performed at different excitation wavelengths along the low energy component of the $^4I_{9/2} \rightarrow {}^4F_{3/2}$ absorption band show that the lifetime displays a variation of about a 20% and does not show a monotonic variation with wavelength. This behavior is observed in all samples studied. As an example Fig. 4 shows the excitation wavelength dependence of the lifetimes for glass GPB2. As can be observed, the lifetime initially decreases with increasing wavelength but after reaching a minimum it increases again (this lifetime increasing at long wavelengths could be attributed to the presence of a variety of different centers and/or the existence of energy transfer). The wavelength dependence suggests large site-to-site differences in the local crystal field. The same behavior was found at 4.2 K. The lifetime values are nearly independent of temperature in the 4.2–300 K range for all samples.

TABLE III. Room temperature emission properties of Nd^{3+} in bismuth lead-germanate glasses. The radiative lifetime of the $^4F_{3/2}$ state has been estimated by using the Judd-Ofelt parameters.

Glass	n	λ_p (nm)	$\Delta\lambda_{\text{eff}}$ (nm)	σ_p (10^{-20} cm^2)	τ_R (μs)	τ_{exp} (μs)
GP	1.959	1063.7	26.1	4.4	176	182
GPB1	2.021	1065	27.6	4.1	180	172
GPB2	2.033	1065	27.2	4.6	155	166
GPB3	2.012	1064.2	26.8	4.9	142	158
GPB4	2.003	1064	26.5	4.3	164	154
GB	1.945	1064.7	28.1	4.6	173	172

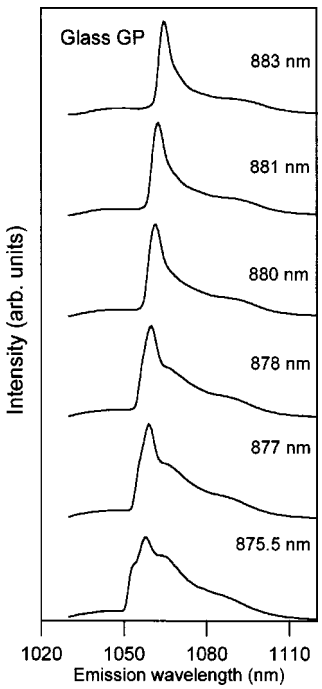

FIG. 3. Steady-state emission spectra of transition $^4F_{3/2} \rightarrow {}^4I_{11/2}$ in glass GP for different excitation wavelengths along the low energy Stark component of the $^4F_{3/2}$ level. Data correspond to 4.2 K.

C. Time-resolved fluorecence line-narrowing spectra

The characteristic spectroscopic feature of rare-earth ions in glass is the inhomogeneous broadening resulting from the distribution of the crystal fields at the variety of rare-earth-ion sites in the amorphous solid.[17] Inhomogeneous broadening influences substantially the lasing processes that occur in the medium. To understand these processes it is important to investigate the interaction between monochromatic radiation and an assembly of spectrally inhomogeneous active centers. One of the most important factors is the migration of the electron excitation over the inhomogeneous profile (spectral migration), which determines the effectiveness of the generation (amplification) of the stimulated emission.[17] One of the kinetic methods of migration investigation consists in analyzing time-resolved luminescence spectra after selective excitation.[17–21,30,31] The TRFLN technique provides us with a way of measuring optical energy propagation from the initially excited subset of ions to other elements of the inhomogeneously broadened line. Therefore, the existence of energy transfer among Nd^{3+} ions in these glasses can be studied by using TRFLN spectroscopy and observing the emission characteristics of the system as a function of time. Previous works[17–19] on Nd-doped glasses utilized a nonresonant pumping scheme to excite the $^4F_{3/2}$ state which is responsible for the principal Nd^{3+} fluorescence. Under the nonresonant pumping condition the ''accidental coincidence'' effect influences the originating state of the fluorescence in a complicated way and hence no direct analysis can be made of the TRFLN donor-donor dynamics in such cases.[32] The introduction of tunable lasers for resonant excitation in the near infrared made it possible to perform measurements on TRFLN under resonant excitation of the $^4F_{3/2}$ state of Nd^{3+} to study the structure of inhomogeneously broadened bands and migration of excitation energy among Nd^{3+} ions.[20,21,33] In this work, TRFLN spectra for the $^4F_{3/2} \rightarrow {}^4I_{9/2}$ transition were performed for all samples between 4.2 and 150 K by using different resonant excitation wavelengths in the low energy Stark component of the $^4I_{9/2} \rightarrow {}^4F_{3/2}$ absorption band at different time delays after the laser pulse. Typical results from these measurements are given in Fig. 5, which shows the normalized $^4F_{3/2} \rightarrow {}^4I_{9/2}$ spectra at 4.2 K for glass GP obtained at two different time delays after the laser pulse, 1 and 350 μs, by exciting at the low energy Stark component of the $^4I_{9/2} \rightarrow {}^4F_{3/2}$ absorption band. Two contributing components can be observed in the spectra. The component observed on the high energy side of the line is a simple FLN line (linewidth ≈ 8 cm^{-1}) corresponding to the emission to the lowest component of the $^4I_{9/2}$ multiplet, which is the ground state of the ion. The position of this narrow line is essentially determined by the wavelength of the pumping radiation. The broad emission arises from the non-narrowed inhomogeneous line. As time delay increases the relative intensity of the narrow line and the broad (nonselected) emission changes, and the later becomes stronger, which indicates the existence of energy transfer between discrete regions of the inhomogeneous broadened profile.

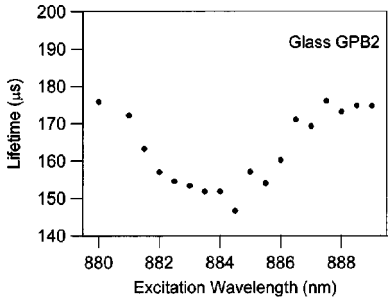

FIG. 4. Lifetimes of the $^4F_{3/2}$ state in glass GPB2 as a function of excitation wavelength along the $^4I_{9/2} \rightarrow {}^4F_{3/2}$ absorption band. Data correspond to 77 K.

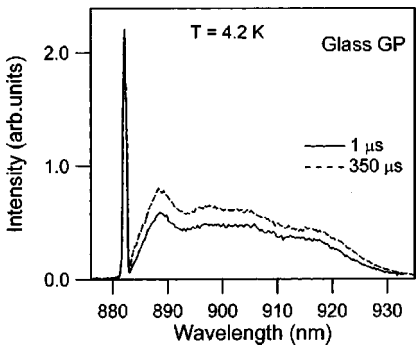

FIG. 5. Time resolved fluorescence line narrowed spectra of the $^4F_{3/2} \rightarrow {}^4I_{9/2}$ transition in glass GP obtained from excitation at 882 nm at two different time delays after the laser pulse. Data correspond to 4.2 K.

The $^4F_{3/2} \rightarrow {}^4I_{9/2}$ spectra were also performed by exciting at different wavelengths along the low energy Stark component of the $^4I_{9/2} \rightarrow {}^4F_{3/2}$ absorption band. Figure 6 shows the normalized $^4F_{3/2} \rightarrow {}^4I_{9/2}$ spectra at 4.2 K for glass GPB2 obtained at two different time delays after the laser pulse, 1 μs and 1 ms, and at three different excitation wavelengths. The

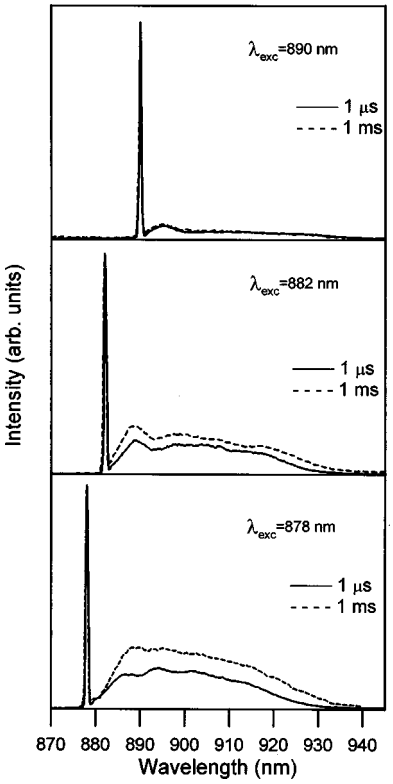

FIG. 6. Time resolved fluorescence line narrowed spectra of the $^4F_{3/2} \rightarrow {}^4I_{9/2}$ transition in glass GPB2 obtained at 1 μs and 1 ms after the laser pulse at different excitation wavelengths. Measurements correspond to 4.2 K.

pattern of these spectra reveals that the broad emission decreases as the excitation energy decreases, which indicates that excitation energy can migrate mainly in one direction.[30]

The time evolution of laser-induced resonant line-narrowed fluorescence is produced by a combination of radiative decay and nonradiative transfer to other nearby ions. Subsequent fluorescence from the acceptor ions replicate the inhomogeneously broadened equilibrium emission profile, showing that transfer occurs not to resonant sites but to the full range of sites within the inhomogeneous profile. In this case, a quantitative measure of the transfer is provided by the ratio of the intensity in the narrow line to the total intensity of the fluorescence in the inhomogeneous band.

Neglecting the dispersion in the radiative decay rate, and using the Föster formula for dipole-dipole energy transfer, one can write for the relationship between the integral intensities of the broad background emission I_B and the narrow luminescence component I_N.

$$\ln\left(\frac{I_B}{I_N}+1\right)=\gamma(E_L)t^{1/2}. \tag{1}$$

The macroscopic parameter $\gamma(E_L)$ has the meaning of an integral characteristic, which reflects the average rate of excitation transfer from donors to the ensemble of spectrally nonequivalent acceptors.[30]

This analysis deals with migration induced changes in an individual luminescence band originating from transitions between a pair of Stark sublevels.[30] However, in the case of Nd^{3+} ions, the luminescence spectra represent a superposition of different Stark components. At low temperature, where only the lowest Stark sublevels of the ground and metastable states are populated, the spectra show a narrow resonant Stark component and some broad emission due to transitions to the other Stark components of the ground state, whereas at higher temperatures the spectral pattern becomes more complicated. As a consequence, though at high temperatures spectral migration can be experimentally observed, the analysis in terms of Eq. (1) which considers a two-level scheme becomes more complicated.

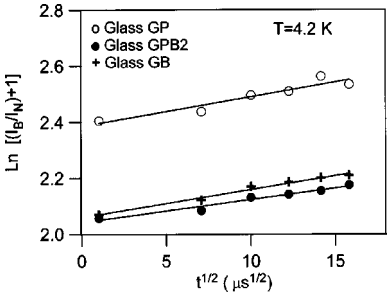

FIG. 7. Analysis of the time evolution of the TRFLN $^4F_{3/2} \rightarrow {}^4I_{9/2}$ emission by means of Eq. (1) for three different samples. Symbols correspond to experimental data and the solid lines are fits to Eq. (1). Data correspond to 4.2 K.

We have analyzed the TRFLN spectra of the transition $^4F_{3/2} \rightarrow {}^4I_{9/2}$ obtained at different time delays between 1 and 350 μs according to Eq. (1) at 4.2 K. As as example, Fig. 7 shows the results for glasses GP, GPB2, and GB doped with 1 mol % of Nd^{3+} at 4.2 K for an excitation wavelength of 882 nm. As can be observed a linear dependence of the $\ln[(I_B/I_N+1)]$ function on $t^{1/2}$ was found, indicating that a dipole-dipole interaction mechanism among the Nd^{3+} ions dominates in this time regime. The values of the average transfer rate indicate that energy transfer among Nd^{3+} ions is weak at this concentration and temperature. As temperature increases a change in the intensity of both components of the spectra is observed. The narrow line broadens and decreases its intensity whereas the one of the broad component increases. The analysis of the TRFLN spectra obtained at different time delays at 77 K also shows a linear dependence of the $\ln(I_B/I_N+1)$ function on $t^{1/2}$ and an increase in the transfer rate.

D. Infrared to visible upconversion

Frequency upconversion by resonantly pumped rare-earth doped materials has received increasing attention in recent years. In conventional oxide glasses the upconversion efficiency is considered to be low because of a large multiphonon relaxation rate due to the high energy phonons. However, in lead-germanate glasses the reduced phonon energy should increase the upconversion efficiency. Infrared to visible upconversion in an Er^{3+}-doped calcium lead-germanate glass has been reported by Pan *et al.*[7] and more recently, orange-blue frequency upconversion in a Pr^{3+}-doped lead germanate glass has been reported by the authors.[34]

In this work, visible upconversion has been observed in these bismuth-lead-germanate glasses doped with 1 mol % of Nd^{3+} under continuous wave (cw) and pulsed laser excita-

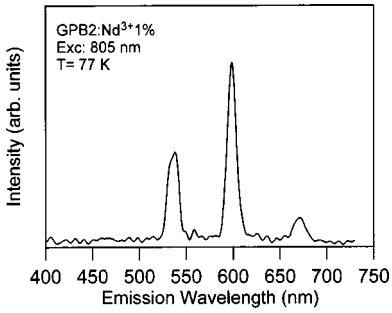

FIG. 8. Upconversion emission spectrum for glass GPB2 obtained under cw excitation at 805 nm at 77 K.

tion. The samples were pumped in the 780–920 nm spectral range by using a Ti-sapphire ring laser (0.4 cm^{-1} linewidth) and a Ti-sapphire laser, pumped by a pulsed frequency doubled Nd:YAG laser (9 ns pulse width). A cutoff filter (transmittance 400–750 nm) was used to remove both the pumping radiation and the infrared luminescence from the samples. As an example, Fig. 8 shows the upconversion fluorescence in the 400–750 nm region at 77 K for GPB2 glass obtained by exciting at 805 nm (cw) in resonance with the $^4I_{9/2} \rightarrow {}^4F_{5/2}$ transition. The spectrum shows three main bands centered at around 535, 598, and 671 nm. It is worthy to mention that the intensity of the visible luminescence is weak in the 77–295 K temperature range and can be only measured under high intensity pumping ($\geqslant$ 140 mW on the sample). The dependence of the three lines intensity on the pump power is nearly quadratic (slope 1.6), which indicates a two photon upconversion process.

The energy level diagram shown in Fig. 9 was constructed by using the room temperature absorption spectrum for

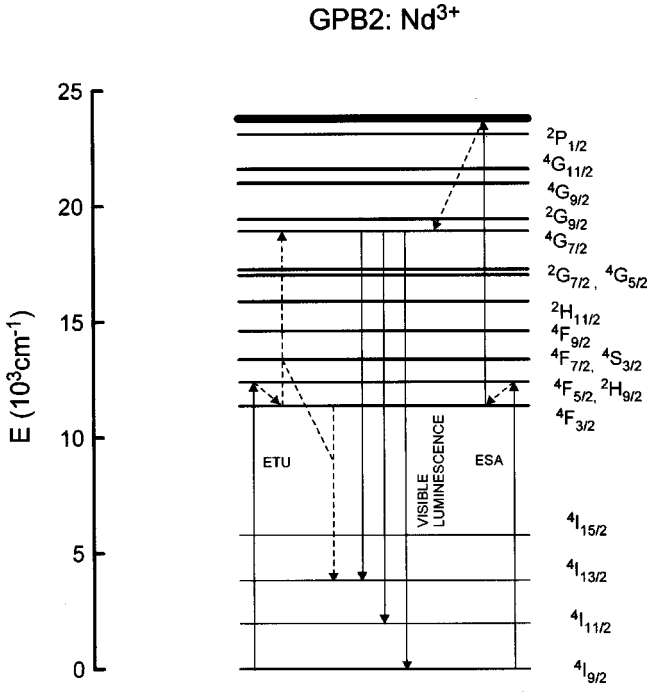

FIG. 9. Energy level diagram for Nd^{3+} in GPB2 glass obtained from the room temperature absorption spectrum. Possible upconversion mechanisms and assignments of the emission bands observed with an 805 nm excitation are also indicated.

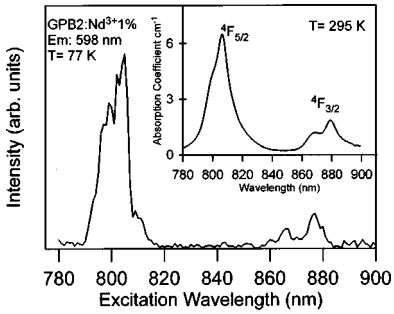

FIG. 10. Excitation spectrum of the 598 nm line, corrected for the spectral variation of the laser intensity. Measurements were performed at 77 K.

GPB2 glass. In this figure we also indicate the two possible mechanisms leading to the observed visible luminescence after infrared excitation.

In order to identify each emission band, we have used the low temperature emission spectrum given in Fig. 8 and the energy level diagram of Nd^{3+} in GPB2 glass shown in Fig. 9. The three bands observed in the emission spectrum have been reported in other Nd-doped materials, and attributed to transitions from the $^4G_{7/2}$ and $^4G_{5/2}$ levels.[35–37] An analysis of the energy level diagram and the emission spectrum suggests that the observed bands can be originated from the $^4G_{7/2}$ level. So the bands can be attributed to transitions $^4G_{7/2} \rightarrow {}^4I_{9/2}$ (535 nm), $^4G_{7/2} \rightarrow {}^4I_{11/2}$ (598 nm), and $^4G_{7/2} \rightarrow {}^4I_{13/2}$ (671 nm). This hypothesis is supported by lifetime measurements performed by exciting at the $^4F_{3/2}$ level with a pulsed Ti-sapphire laser and collecting the luminescence at the peak positions of the visible emission bands. A lifetime value of about 50 μs was found for the three observed emissions.

The excited $^4G_{7/2}$ state can be populated by two possible mechanisms, excited state absorption (ESA) and/or energy transfer (ETU) (see Fig. 9). In the first process (ESA), Nd^{3+} ions in the $^4F_{3/2}$ state, populated upon relaxation from the $^4F_{5/2}$ state, absorb pump photons and are excited to the $^2D_{5/2}$ state, from which they can decay nonradiatively to the $^4G_{7/2}$ state. In the second process (ETU), when two Nd^{3+} ions are excited to the $^4F_{3/2}$ state, a transfer occurs by which one ion loses energy and goes to the $^4I_{13/2}$ state while the other one gains energy and goes to the $^4G_{7/2}$ state. These processes can coexist, contributing to the excitation into higher levels. To obtain information about the dominant mechanism responsible for the upconverted luminescence, the excitation spectrum of the visible emissions was investigated in the 780–920 nm range (by using the Ti-sapphire tunability). Similar excitation spectra were obtained by collecting the luminescence at 535, 598, and 671 nm. As an example, the excitation spectrum of the 598 nm band is presented in Fig. 10 together with the absorption spectrum in this spectral range (on the inset) for comparison. As can be observed the excitation spectrum shows the peaks corresponding to the $^4I_{9/2} \rightarrow {}^4F_{5/2}, {}^4F_{3/2}$ absorption bands, without any significant differences with the absorption spectrum. (The slightly narrow and blue shift in the excitation spectrum is because this spectrum was recorded at 77 K.) This behavior indicates that an ETU process seems to be responsible for the observed visible luminescence, though other possible mechanisms can not be disregarded.[35]

IV. CONCLUSIONS

(i) From the steady-state optical absorption measurements the Judd-Ofelt parameters were derived and used to calculate the $^4F_{3/2} \rightarrow {}^4I_{11/2}$ stimulated emission cross section and the $^4F_{3/2}$ radiative lifetime for Nd^{3+} in six samples with a different composition. The smallest value of the Ω_2 parameter for glass GP suggests a more centrosymmetric coordination environment for the Nd^{3+} ions. The narrowest effective linewidth of the $^4F_{3/2} \rightarrow {}^4I_{11/2}$ transition corresponds to glass GP, increasing as the bismuth oxide concentration increases in the glass composition. The highest stimulated emission cross-section which is determined by Ω_4 and Ω_6 and the effective fluorescence linewidth corresponds to glass GPB3.

(ii) The narrowing observed in the steady-state emission spectra of the $^4F_{3/2} \rightarrow {}^4I_{11/2}$ transition when the exciting wavelength increases along the $^4I_{9/2} \rightarrow {}^4F_{3/2}$ absorption band, together with the nonmonotonic dependence of the lifetimes on the excitation wavelength, reveal the existence of a broad distribution of Nd^{3+} sites in these glasses. The spectral features and inhomogeneous broadening of the emission spectra for the glasses studied suggest that the addition of Bi_2O_3 contributes to a greater variation in the local crystal field.

(iii) Analysis of the time evolution of the $^4F_{3/2} \rightarrow {}^4I_{9/2}$ emission spectra obtained at low temperature under resonant excitation shows that spectral migration of excitation among neodymium ions is weak at 1 mol % Nd^{3+} concentration and can be interpreted in terms of dipole-dipole energy transfer.

(iv) The observed behavior for the visible emission obtained under infrared excitation suggests that an ETU process are responsible for the unconverted luminescence, though other possible mechanisms can not be disregarded.

ACKNOWLEDGMENTS

This work has been supported by the Spanish Government CICYT (Ref. MAT97-1009), (DGICYT Ref. PB95-0512), and Basque Country University (G21/98).

[1] W. H. Dumbaugh, Phys. Chem. Glasses **27**, 119 (1986).
[2] J. E. Shelby, J. Am. Ceram. Soc. **71**, C254 (1988).
[3] D. W. Hall, M. A. Newhouse, N. F. Borrelli, W. M. Dumbaugh, and D. L. Weidman, Appl. Phys. Lett. **54**, 1293 (1989).
[4] H. Takebe, K. Yoshino, T. Murata, K. Morinaga, J. Hector, W. S. Brocklesby, D. W. Hewak, J. Wang, and D. N. Payne, Appl. Opt. **36**, 5839 (1997).
[5] D. Lezal, J. Pedlíková, and J. Horák, J. Non-Cryst. Solids **196**, 178 (1996).
[6] J. Wang, J. R. Lincoln, W. S. Brocklesby, R. S. Deol, C. J. Mackechnie, A. Pearson, A. C. Tropper, D. C. Hanna, and D. N. Payne, J. Appl. Phys. **73**, 8066 (1993).
[7] Z. Pan, H. Morgan, A. Loper, V. King, B. H. Long, and W. E. Collins, J. Appl. Phys. **77**, 4688 (1995).
[8] J. McDougall, D. B. Hollis, and M. J. P. Payne, Phys. Chem. Glasses **36**, 52 (1995).
[9] D. P. Shepherd, D. J. B. Brick, J. Wang, A. C. Tropper, D. C. Hanna, G. Kakarantzas, and P. D. Twonsend, Opt. Lett. **19**, 954 (1994).
[10] M. Wachtler, A. Speghini, K. Gatterer, H. P. Fritzer, D. Ajò, and M. Bettinelli, J. Am. Ceram. Soc. **81**, 2045 (1998).
[11] A. E. Miller, K. Nassau, K. B. Lyons, and M. E. Lines, J. Non-Cryst. Solids **99**, 289 (1988).
[12] J. E. Canale, R. A. Condrate, K. Nassau, and B. C. Cornilsen, J. Can. Ceram. Soc. **55**, 50 (1986).
[13] M. J. Weber, J. Non-Cryst. Solids **123**, 208 (1990).
[14] M. J. Weber, in *Laser Spectroscopy of Solids*, edited by W. M. Yen and P. M. Selzer, Topics in Applied Physics Vol. 49, (Springer, Berlin, 1981), pp. 189–239, and references therein.
[15] R. Balda, J. Fernández, J. L. Adam, and M. A. Arriandiaga, Phys. Rev. B **54**, 12 076 (1996).
[16] S. E. Stokowski, in *Lasers, Spectroscopy and New Ideas*, edited by W. M. Yen and M. D. Levenson, Springer Series in Optical Sciences Vol. 54 (Springer, Berlin, 1987), p. 47.
[17] L. A. Riseberg, Phys. Rev. A **7**, 671 (1973).
[18] L. D. Merkle, R. C. Powell, and E. E. Freed, J. Lumin. **24/25**, 755 (1981).
[19] L. A. Riseberg, Solid State Commun. **11**, 469 (1972).
[20] T. T. Basiev, Yu K. Voron'ko, S. B. Mirov, and A. M. Prokhorov, Pis'ma Zh. Eksp. Teor. Fiz. **29**, 696 (1979) [JETP Lett. **29**, 639 (1979)].
[21] S. A. Brawer and M. J. Weber, Appl. Phys. Lett. **35**, 31 (1979).
[22] X. Liu, D. B. Hollis, and J. McDougall, Phys. Chem. Glasses **37**, 160 (1996).
[23] B. R. Judd, Phys. Rev. **127**, 750 (1962).
[24] G. S. Ofelt, J. Chem. Phys. **37**, 511 (1962).
[25] R. R. Jacobs and M. J. Weber, IEEE J. Quantum Electron. **QE12**, 102 (1976).
[26] H. Takebe, K. Morinaga, and T. Izumitani, J. Non-Cryst. Solids **178**, 58 (1994).
[27] C. K. Jorgensen and R. Reisfeld, J. Less-Common Met. **93**, 107 (1983).
[28] W. F. Krupke, IEEE J. Quantum Electron. **QE10**, 450 (1974).
[29] M. J. Weber, J. D. Myers, and D. H. Blackburn, J. Appl. Phys. **52**, 2944 (1981).
[30] T. T. Basiev, V. A. Malyshev, and A. K. Prhevuskii, in *Spectroscopy of Solids Containing Rare Earth Ions*, edited by A. A. Kaplyanskii and R. M. Macfarlane (North-Holland, Amsterdam 1987), p. 303, and references therein.
[31] O. K. Alimov, T. T. Basiev, Yu K. Voron'ko, L. S. Gaigerova, and A. V. Dmitryuk, Zh. Eksp. Teor. Fiz. **72**, 1313 (1977) [Sov. Phys. JETP **45**, 690 (1977)].
[32] W. M. Yen, in *Spectroscopy of Solids Containing Rare Earth Ions* (Ref. 30), p. 185.
[33] M. M. Broer, D. L. Huber, W. M. Yen, and W. K. Zwicker, Phys. Rev. Lett. **49**, 394 (1982).
[34] R. Balda, J. Fernández, A. de Pablos, and J. M. Fdez-Navarro, J. Phys.: Condens. Matter **11**, 7411 (1999).
[35] A. T. Stanley, E. A. Harris, T. M. Searle, and J. M. Parker, J. Non-Cryst. Solids **161**, 235 (1993).
[36] T. Tsuneoka, K. Kojima, and S. Bojja, J. Non-Cryst. Solids **202**, 297 (1996).
[37] T. Chuang and H. R. Verdún, IEEE J. Quantum Electron. **32**, 79 (1996).